Neuron, Vol. 42, 51–62, April 8, 2004, Copyright ©2004 by Cell Press

Lipid Rafts Mediate Chemotropic Guidance of Nerve Growth Cones

Carmine Guirland,[1] Shingo Suzuki,[2] Masami Kojima,[2] Bai Lu,[3] and James Q. Zheng[1,*]
[1]Department of Neuroscience and Cell Biology
University of Medicine and Dentistry of New Jersey
Robert Wood Johnson Medical School
Piscataway, New Jersey 08854
[2]Division for Life Science Technology
National Institute of Advanced Industrial Science and Technology
Ikeda, Osaka 563-8577
Japan
[3]Section on Synapse Development & Plasticity
National Institute of Child Health & Human Development
National Institutes of Health
Bethesda, Maryland 20892

Summary

Axon guidance requires signal transduction of extracellular cues through the plasma membrane for directional motility. Here we present evidence that cholesterol- and sphingolipid-enriched membrane microdomains (lipid rafts) mediate specific guidance responses of nerve growth cones. Disruption of lipid rafts by various approaches targeting cholesterol or gangliosides selectively abolished growth cone attraction and repulsion in BDNF and netrin-1 gradients, respectively, without affecting glutamate-induced attraction. Interestingly, local raft disruption on one side of the growth cone in bath BDNF or netrin-1 produced opposite turning responses to that induced by the gradients. Raft manipulation also blocked Semaphorin 3A-induced growth cone repulsion, inhibition, and collapse. Finally, guidance responses appeared to involve raft-dependent activation of p42/p44 MAPK and ligand-induced receptor recruitment to lipid rafts. Together with the observation of asymmetric receptor-raft associations at the growth cone in guidance gradients, our findings indicate that localized signaling through membrane rafts plays a role in mediating guidance actions of extracellular cues on developing axons.

Introduction

During development, axonal growth is regulated and guided by extracellular cues that elicit permissive/attractive and inhibitory/repulsive effects on the directional motility of axonal growth cones (Tessier-Lavigne and Goodman, 1996). In adult nervous systems, inhibitory/repulsive molecules present a major obstacle for nerve regeneration after injury and diseases (McKerracher and Winton, 2002). Thus, understanding signal transduction mechanisms underlying specific actions of these extracellular cues on nerve growth and guidance will not only enhance our understanding of brain development but also provide potential strategies to combat growth inhibition of regenerating nerve fibers. For many guidance cues, the formation of ligand-receptor complexes on the plasma membrane represents the first step in signal transduction, followed by additional events such as receptor oligomerization and complex formation with coreceptors and/or other membrane-associated components (Huber et al., 2003). For example, it was recently shown that cross-talk between different guidance receptors specifically enables a particular response while silencing another (Stein and Tessier-Lavigne, 2001). The fact that these important events occur at or within the plasma membrane suggests that the membrane lipid environment is crucial for signal transduction of these extracellular cues. Whether or not a specific lipid environment of the plasma membrane plays a role in guidance signaling, however, remains unknown. While the membrane components involved in receptor-signaling complexes are currently being identified, how these receptors and other components interact on the membrane to generate specific signaling cascades for distinct axonal responses remains elusive.

Recent studies indicate that the plasma membrane contains dynamic microdomains that are enriched with cholesterol and glycosphingolipids, resistant to cold detergent extraction, and of lower buoyant density than bulk plasma membrane (Brown and London, 1998; Simons and Toomre, 2000). Known collectively as lipid rafts, these membrane domains are also enriched with certain membrane proteins such as caveolins, src-family kinases, and glycosylphosphatidylinositol (GPI)-anchored proteins (Brown and London, 1998; Simons and Toomre, 2000). Although only a limited number of transmembrane proteins are known to associate with lipid rafts, they are of significance as many are receptors for extracellular signals, including those involved in axon elongation and guidance (Tsui-Pierchala et al., 2002). It is believed that lipid rafts provide suitable microenvironments to enable selective protein-protein interactions as well as local initiation of signal transduction (Simons and Toomre, 2000; Tsui-Pierchala et al., 2002). An increasing number of recent studies indicate that lipid rafts play important roles in many cellular responses to extracellular signals, including growth factor effects and immune responses (Brown and London, 1998; Simons and Toomre, 2000). So far, only a few guidance molecules and receptors have been examined and shown to associate with lipid rafts, and there is no direct evidence indicating a major role for lipid rafts in axon guidance (Tsui-Pierchala et al., 2002). In this study, we examined the role of lipid rafts in chemotropic guidance of nerve growth cones by diffusible gradients of brain-derived neurotrophic factor (BDNF), netrin-1, Semaphorin 3A (Sema3A), and glutamate. Using an in vitro functional assay for guidance responses combined with complementary approaches of raft manipulation, we show that distinct guidance responses of nerve growth cones to BDNF, netrin-1, and Sema3A, but not glutamate, depend on the integrity of lipid rafts. We further provide data that local signaling

*Correspondence: james.zheng@umdnj.edu

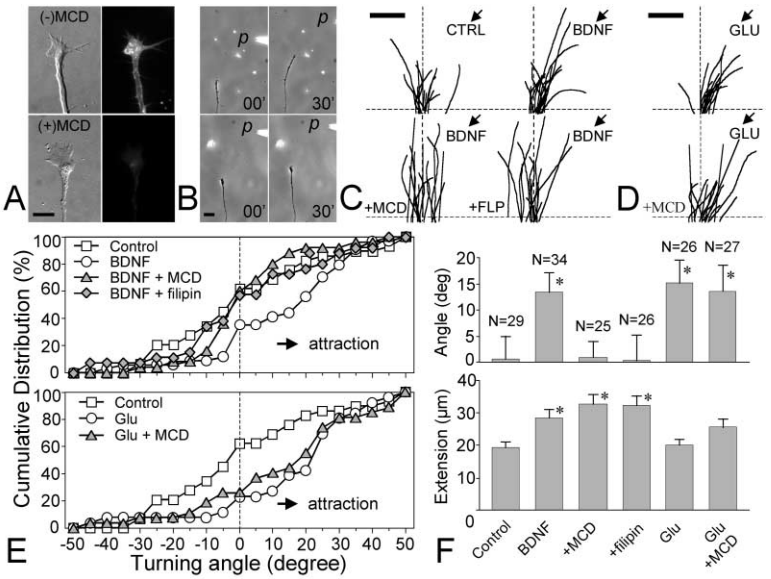

Figure 1. Lipid Raft Disruption by Cholesterol Manipulation Selectively Abolishes BDNF-Induced Growth Cone Attraction

(A) DIC (left) and fluorescence (right) images of cultured *Xenopus* growth cones labeled with filipin for visualizing membrane cholesterol, without (−) and with (+) MCD treatment (5 mM, 30 min). Scale bar equals 10 μm.

(B) Growth cone turning in BDNF gradients without (top pair) or with (bottom pair) 5 mM MCD in bath saline. Digits depict the time after the onset of the BDNF gradient. P indicates the BDNF pipette.

(C) Superimposed traces of the trajectory of neurite extension during the 30 min turning assay of 15 representative cells for each condition. The origin is the center of the growth cone at the onset of the gradient; the original direction of growth cone extension was vertical. Arrows indicate the direction of the gradient.

(D) Growth cone attraction induced by glutamate gradients without (top) and with (bottom) 5 mM MCD in the bath.

(E) Cumulative histograms showing the distribution of the turning angles for each condition. Each point represents the percentage of growth cones with final turning angles equal to or less than the values indicated on the abscissa. Top: turning induced by BDNF gradients; bottom: turning induced by glutamate gradients.

(F) Average turning angles (top) and net extension (bottom) of different groups of all the growth cones examined. Numbers indicate the total number of growth cones examined for each condition.

Scale bars in (B)–(D) equal 20 μm. Abbreviations: CTRL, control medium; FLP, filipin; GLU, glutamate. Treatments were added to the bath 20–30 min prior to either fixation (A) or turning assays (C–F). MCD and FLP were used at 5 mM and 0.1 μg/ml, respectively. Asterisks indicate significance when compared to the control ($p < 0.01$, Mann-Whitney test).

through lipid rafts underlies growth cone responses to these guidance cues. Finally, we demonstrate a guidance cue-induced recruitment of specific receptors to lipid rafts and asymmetric receptor-raft association on the growth cone surface in guidance gradients. These findings thus indicate a functional role for lipid rafts in mediating localized signal transduction during growth cone guidance.

Results

Disruption of Lipid Rafts Selectively Blocks Growth Cone Attraction by BDNF

Embryonic *Xenopus* neurons cultured on laminin were used in the turning assay to examine chemotropic responses of growth cones to a number of guidance cues (Guirland et al., 2003). We manipulated the integrity of lipid rafts using methyl-β-cyclodextrin (MCD), a water-soluble cyclic oligomer that extracts cholesterol from the plasma membrane (Simons and Toomre, 2000). Incubation of *Xenopus* neurons with a relatively low concentration of MCD (5 mM) for 30 min largely depleted membrane cholesterol without significantly affecting the growth cone motility and morphology, as examined by light microscopy and fluorescent staining of membrane cholesterol with filipin, a polyene antibiotic that binds to membrane cholesterol (Figure 1A; Robinson and Karnovsky, 1980). We first investigated the effects of cholesterol extraction by MCD on BDNF-induced growth cone attraction using the standard in vitro turning assay (Ming et al., 1997; Song et al., 1997). We found that a gradient of BDNF (50 μg/ml in the ejection pipette, ~50 ng/ml reaching the growth cone) induced marked attraction of *Xenopus* growth cones within 30 min of the gradient application, whereas acute MCD treatment abolished the attractive response (Figure 1B). Composite traces of the trajectories of 15 randomly selected growth cones from each group further confirm the abolition of BDNF-induced attraction by MCD treatment (Figure 1C). While the majority of growth cones exposed to the BDNF gradient extended toward the BDNF pipette, MCD-treated growth cones did not exhibit any directional preference in the BDNF gradient (Figure 1C). The elimination of BDNF-induced attraction by MCD raft disruption is best depicted by the cumulative distributions of turning angles (Figure 1E): growth cones exposed only to BDNF gradients displayed a distribution shifted to the positive territory, while MCD-treated growth cones exhibited a distribution overlapped with that of the control group. The effects of MCD raft disruption on BDNF guidance are summarized by the average turning angles (Figure 1F) of all growth cones. While the BDNF gradient induced significant attraction relative to the control group (average turning angles ± SEM, 13.2° ± 3.7° and 0.6° ± 4.4°, respectively; $p < 0.01$, Mann-Whitney test), no preferential turning was observed for growth cones treated with MCD (average turning angles, 0.9° ± 3.1°; $p > 0.5$, Mann-Whitney test). To assure that the blockade of BDNF-induced attraction is not an artifact of membrane cholesterol depletion by MCD, we also disrupted lipid rafts using filipin, which is structurally different from MCD and does not deplete cholesterol from the membrane (Simons and Toomre, 2000). Consistently, BDNF-induced growth cone attraction was also abolished by bath application of 0.1 μg/ml filipin (Figures 1C, 1E, and 1F). Statistical comparison of turning angles among the control, MCD-treated, and filipin-treated

groups shows no difference ($p > 0.5$, Mann-Whitney test), further confirming the effective elimination of the BDNF attractive effects by either MCD or filipin treatment.

To determine that MCD or filipin abrogation of BDNF-induced attraction is not due to their nonspecific actions on growth cone motility, we examined growth cone turning induced by glutamate gradients since it is mediated by Ca^{2+} signals through NMDA channels (Zheng et al., 1996), which are not associated with lipid rafts (Suzuki et al., 2001; Wu et al., 1997). Consistently, a glutamate gradient (50 mM in pipette, ~50 μM reaching the growth cone) induced marked attraction of *Xenopus* growth cones on laminin. Unlike BDNF, however, glutamate-induced attraction was not affected by cholesterol extraction using 5 mM MCD as evidenced by composite traces (Figure 1D), cumulative distributions (Figure 1E), and average turning angles (Figure 1F). Both groups exposed to glutamate gradients (−MCD and +MCD) exhibited similar average turning angles (15.0° ± 4.4° and 13.5° ± 4.9°, respectively; $p > 0.5$, Mann-Whitney test), which are significantly different from that of the control ($p < 0.01$). These results provide direct evidence that lipid raft disruption by cholesterol manipulation did not impair the growth cone's ability to advance, sense, and respond to guidance gradients per se, but selectively blocked BDNF-induced attraction. Taken together, our data indicate that the integrity of lipid rafts is required for chemoattractive effects of BDNF gradients.

Growth Cone Guidance by Netrin-1 Depends on Lipid Rafts

Netrin-1 is a well-established guidance cue that attracts as well as repels nerve growth cones in vivo (Tessier-Lavigne and Goodman, 1996), so we examined the raft involvement in netrin-1 guidance in vitro. Under the same culture and assay conditions as above, netrin-1 gradients (5 μg/ml in pipette, ~5 ng/ml at the growth cone) significantly repelled *Xenopus* growth cones on laminin (Figure 2A), which is consistent with previous reports that young *Xenopus* spinal neurons were repelled by netrin-1 (Buck and Zheng, 2002; Ming et al., 2001) and laminin favored netrin-1 repulsion for *Xenopus* retinal neurons (Hopker et al., 1999). The cumulative distribution of turning angles shows that a larger percentage of growth cones exhibit negative turning angles (Figure 2C), producing an average of −18.0° ± 5.4° (Figure 2D; $p < 0.01$, compared to the control group shown in Figure 1). However, bath application of 5 mM MCD completely abolished the repulsion (Figure 2B), resulting in an angle distribution centering at zero (Figure 2C) and an average of 2.3° ± 5.0° (Figure 2D; $p > 0.5$, compared to the control group). We also found that bath application of 0.1 μg/ml filipin blocked the growth cone repulsion induced by netrin-1 gradients (Figures 2C and 2D). The net neurite extension was not significantly affected by either MCD or filipin treatment ($p > 0.5$). Based on these findings, we conclude that the integrity of lipid rafts is also crucial for netrin-1 signaling in growth cones. Together with the inhibition of BDNF-induced attraction by lipid raft disruption, our data indicate that cholesterol-enriched membrane domains, i.e., lipid rafts, play an important role in both attractive and repulsive guidance of nerve growth cones by BDNF and netrin-1, respectively.

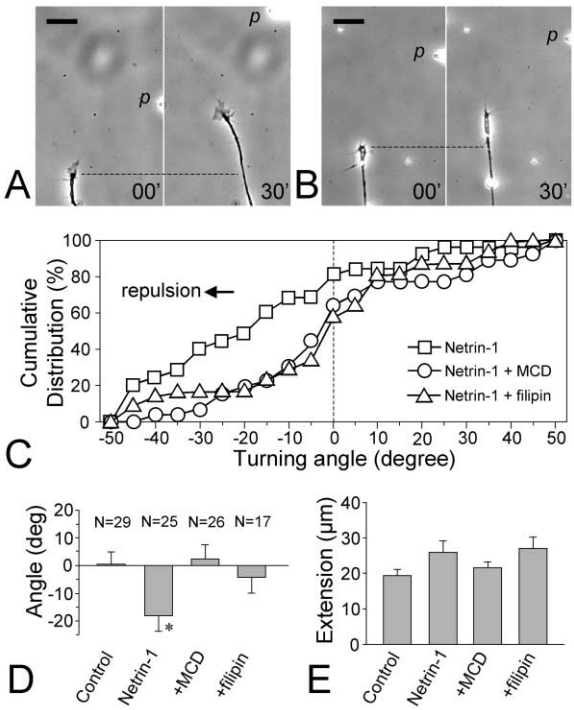

Figure 2. Growth Cone Turning Induced by Netrin-1 Depends on Lipid Raft Integrity

(A and B) Representative images showing *Xenopus* growth cones at the onset and the end of 30 min exposure to a netrin-1 gradient (5 μg/ml in pipette) without (A) and with (B) 5 mM MCD in bath. Dashed lines represent the corresponding positions of the growth cone at the onset of the turning assay. Scale bars equal 20 μm.

(C) The cumulative histogram depicts the responses to netrin-1 gradients without or with lipid raft disruption by 5 mM MCD or 0.1 μg/ml filipin.

(D and E) Average turning angles (D) or net extension (E) for each condition are depicted by bar graphs, and the total numbers of growth cones examined for each condition are indicated in (D). Asterisks indicate significance over the control ($p < 0.01$, Mann-Whitney test).

Further Evaluation of Raft Dependence of Growth Cones' Responses to BDNF and Netrin-1

The above findings were all based on cholesterol manipulation for lipid raft disruption. Cholesterol extraction by MCD was shown to partially release certain protein components from the plasma membrane (Ilangumaran and Hoessli, 1998), which could contribute to the blockade of BDNF and netrin-1 guidance reported above. Although our immunostaining found no detectable change in the level of either TrkB or DCC receptors at the growth cone after MCD cholesterol extraction (data not shown), we performed additional experiments to address this issue. We first performed a "rescue" experiment in which *Xenopus* neurons were depleted of cholesterol by a 30 min MCD treatment followed by readdition of a low concentration of cholesterol (cholesterol/MCD complex) and then turning assays. We found that readdition of 20 μM cholesterol (balanced by 160 μM

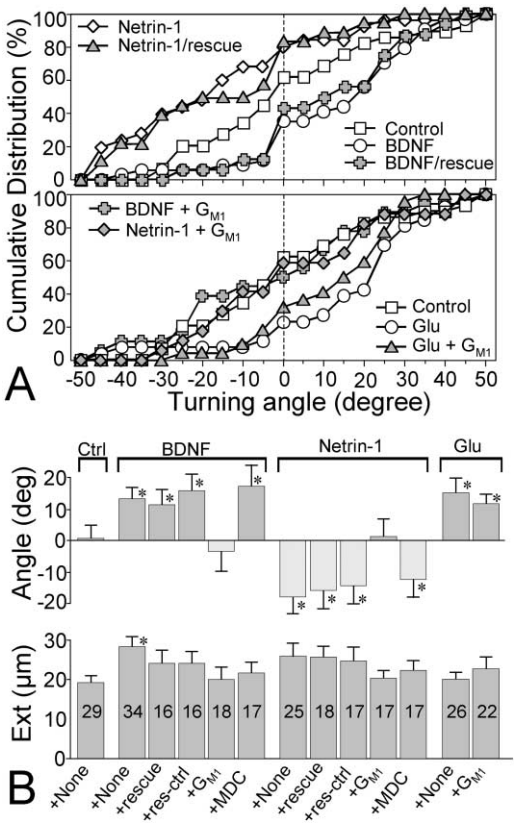

Figure 3. Growth Cone Responses to BDNF or Netrin-1 Selectively Depend on Membrane Lipid Environment

(A) Cumulative histograms depict the turning responses of *Xenopus* growth cones in BDNF, netrin-1, or glutamate gradients under the "rescue" condition (top) or exogenous G_{M1} application (bottom). The "rescue" experiments involved 30 min cholesterol extraction by 5 mM MCD followed by addition of 20 μM cholesterol (with 160 μM MCD). Res-ctrl: growth cones exposed to 20 μM cholesterol (with 160 μM MCD) without prior extraction. For G_{M1} experiments, 20 μM G_{M1} was added to the bath medium 30 min before the turning assays. (B) Average turning angle and net extension of each condition are depicted by the bar graph, and the numbers denote sample size for each experiment. Asterisks indicate significance over the control group ($p < 0.01$, Mann-Whitney test). MDC (monodansylcadaverine) was used at 50 μM.

MCD) immediately restored BDNF-induced attraction (Figure 3). The cumulative distribution of turning angles of "rescued" growth cones essentially overlaps with that of untreated growth cones in the BDNF gradient, both showing marked attraction (Figure 3A). The average turning angle of cholesterol-rescued growth cones to BDNF gradients is 11.1° ± 4.7°, which is significantly different from the control group ($p < 0.05$) but similar to the growth cones exposed only to BDNF gradients ($p > 0.5$). Similarly, we found that netrin-1-induced repulsion was also restored in the similar rescue experiments (Figures 3A and 3B). As an important control, 20 μM cholesterol (balanced by 160 μM MCD) itself did not affect normal turning responses to BDNF and netrin-1, respectively (marked as "res-ctrl," Figure 3B), further supporting the specificity of the rescue experiments. These results thus indicate that cholesterol extraction blocked the guidance effects of BDNF and netrin-1 by mainly affecting the integrity of lipid microenvironments, rather than by stripping away guidance receptors and other protein components from the plasma membrane.

While the above results clearly indicate the involvement of membrane cholesterol in growth cone guidance, the importance of lipid raft integrity is further addressed through a second set of complementary experiments by targeting a different lipid constituent of rafts, the gangliosides. It was previously shown that application of exogenous ganglioside G_{M1} affects the integrity and stability of lipid rafts such that raft-associated proteins are excluded from raft microdomains (Simons et al., 1999). When we added 20 μM G_{M1} to the bath medium prior to the turning assays, BDNF-induced attraction and netrin-1-induced repulsion were all abolished (Figure 3). Statistical analysis shows clearly that exogenous G_{M1} blocked turning responses of *Xenopus* growth cones to BDNF and netrin-1 gradients, respectively ($p > 0.5$ comparing to the control; $p < 0.01$ comparing to respective BDNF and netrin-1 groups without raft manipulation). The selectivity of exogenous G_{M1} on blocking guidance responses to BDNF and netrin-1 was confirmed by the ineffectiveness of G_{M1} to block glutamate-induced growth cone attraction (Figure 3). These results therefore indicate that BDNF and netrin-1 guidance effects depend on lipid rafts. Finally, we have excluded the involvement of clathrin-mediated endocytosis in raft-dependent chemotropic guidance by BDNF and netrin-1. We found that monodansylcadaverine (MDC, 50 μM), a potent inhibitor of clathrin-mediated endocytosis, did not affect BDNF-induced attraction and netrin-1-induced repulsion (Figure 3B). Taken together, results from these complementary studies strongly support the notion that lipid rafts play an essential role in mediating growth cone guidance by BDNF and netrin-1.

Although MCD or filipin treatment abolished BDNF-induced attraction, the growth-promoting effect of BDNF appeared to be largely unaffected. MCD- or filipin-treated growth cones in BDNF gradients still extended more than those exposed to control medium (Figure 1F). On average, growth cones exposed to BDNF gradients with or without cholesterol manipulation extended ~150% of that of the growth cones in control. However, the growth-promoting effects appeared to be abolished by exogenous G_{M1} (Figure 3B), implicating a difference between cholesterol extraction and G_{M1} addition on lipid rafts. To further verify this observation, we performed a growth assay in which randomly selected, isolated neurons were first monitored for 1 hr to determine the net extension of each growth cone. These cells were then exposed to 50 ng/ml BDNF with or without 5 mM MCD or 20 μM G_{M1} for another hour to assess the extension of the same growth cones. For each growth cone, the net extension of the second hour was normalized against that of the first hour to yield the growth ratio (in percentage). Consistently, BDNF exposure significantly increased the neurite extension to 149% ± 21% ($n = 16$) of that in the control hour. Similar enhancement by BDNF was also observed for MCD-treated growth cones (158% ± 22%, $n = 14$), but not G_{M1}-treated cells (97% ± 13%; $n = 10$). Growth cones exposed to the control medium or medium containing MCD or G_{M1} without BDNF exhibited no effects on neurite extension (106% ± 12%, $n = 15$; 93% ± 14%, $n = 15$; and 111% ± 11%,

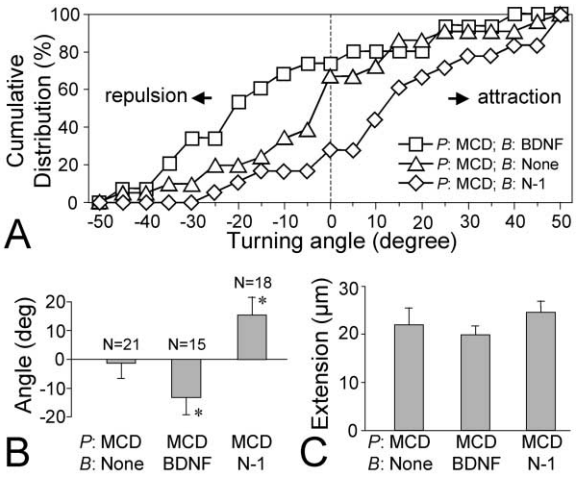

Figure 4. Turning Responses Induced by Local Lipid Raft Disruption in Uniform Guidance Cues

A pipette containing 400 mM MCD (*P*) was placed 50 μm from the growth cone for focal lipid raft disruption (5 ms pulse duration). The growth cones were exposed to bath medium (*B*) containing either BDNF (50 ng/ml) or netrin-1 (5 ng/ml).

(A) The cumulative histogram depicts the responses of growth cones exposed to local MCD with bath medium containing control or BDNF or netrin-1.

(B and C) Average turning angles (B) or net extension (C) for each condition are depicted by bar graphs, and numbers in (B) indicate the total number of growth cones examined for each condition. Asterisks indicate significance when compared to the control ($p < 0.01$, Mann-Whitney test).

$n = 15$, respectively). Statistical analysis using the Student's t test confirms that BDNF significantly increases the extension of *Xenopus* growth cones regardless of MCD treatment ($p < 0.05$). However, such enhancement of extension was eliminated by exogenous G_{M1} addition ($p > 0.5$ comparing to the control groups). These results thus suggest that different aspects of lipid rafts (cholesterol-sensitive and G_{M1}-sensitive) may mediate these distinct effects of BDNF on the growth cone.

Local Signaling through Lipid Rafts Mediates Growth Cone Turning

Chemotropic turning of growth cones in diffusible gradients likely involves asymmetric activation of membrane receptors and localization of intracellular signaling (Hong et al., 2000; Zheng, 2000; Zheng et al., 1994), which may depend on membrane rafts. We thus reasoned that uniform application of these guidance cues in the bath followed by local disruption of lipid rafts on one side of the growth cone would also create an asymmetry in surface receptor activation and downstream signaling across the growth cone. Importantly, however, such asymmetry would be opposite to that induced by the gradient of the same guidance molecule, thus leading to an opposite turning response. We tested this hypothesis by using a focal application method (Buck and Zheng, 2002) to largely restrict MCD to one side of the growth cone. Focal MCD application (400 mM in pipette, ~1 mM reaching the growth cone) in the absence of any guidance molecules in the bath did not affect the direction or the extension rate (Figure 4). However, when 50 ng/ml BDNF was present in the bath, focal MCD application resulted in marked repulsion, contrasting with the attraction induced by a BDNF gradient (Figures 4A and 4B). Conversely, when 5 ng/ml netrin-1 was present in the bath, focal MCD application resulted in a significant attractive turning response (Figures 4A and 4B), which is opposite to the repulsion induced by netrin-1 gradients. No difference in neurite extension was observed for all three groups (Figure 4C), further indicating that local MCD application did not affect the growth cone's normal motility. These results support the notion that asymmetric receptor activation and/or local signaling through lipid rafts underlie growth cone turning responses to guidance gradients.

Lipid Rafts also Mediate Semaphorin 3A Effects on Growth Cones

We also examined turning responses of *Xenopus* neurons to another well-known guidance cue: Semaphorin 3A/collapsin-1 (Sema3A) (Kolodkin et al., 1993). We found that Sema3A gradients exhibited marked inhibition on the extension of *Xenopus* growth cones during turning assays. The majority of growth cones that did advance in Sema3A gradients exhibited marked repulsion, whereas growth cones exposed to pipette application of the vehicle control solution showed no directional preference (Figure 5A). The average turning angles from these two groups highlight the significant repulsion induced by Sema3A (Figure 5B; average angles: $-18.8° \pm 4.1°$ and $1.1° \pm 4.3°$ for the Sema3A and control groups, respectively; $p < 0.01$). Bath application of 5 mM MCD effectively blocked Sema3A-induced repulsion (Figure 5A), resulting in an average turning angle of $6.0° \pm 3.9°$ (Figure 5B; $p > 0.1$ when compared to the control vehicle, Mann-Whitney test). Since only growth cones that extended during the 30 min assay were scored, the neurite extension from our turning assays (Figure 5C) did not reflect Sema3A inhibition on growth cone motility. We therefore performed the growth assay described above to evaluate the role of lipid rafts in growth inhibition by Sema3A. We found that bath application of Sema3A, not the vehicle, significantly inhibited growth cone extension, but such inhibition was largely removed by MCD treatment (Figure 5D). Since Collapsin-1/Sema3A was initially identified for its ability to collapse growth cones, we next examined if lipid rafts are also involved in Sema3A-induced growth cone collapse. Because embryonic *Xenopus* spinal neurons in culture do not exhibit drastic growth cone collapse in response to Sema3A, we used growth cones from basilar pontine explants in culture (Rabacchi et al., 1999) for collapse assays. Consistently, bath application of Sema3A resulted in marked collapse of pontine growth cones as evidenced by the loss of actin-rich lamellipodia and filopodia (Figure 5E). About 80% of the growth cones exhibited collapsed morphology after Sema3A exposure, compared to about 20% in the group exposed to the vehicle ($p < 0.01$, Mann-Whitney test). Disruption of lipid rafts by 1 μg/ml filipin (added 25 min prior to the Sema3A exposure), however, diminished growth cone collapse induced by Sema3A, resulting in a similar collapse percentage to that of the control (Figure 5E; $p > 0.1$, Mann-Whitney test). We could not use MCD for raft disruption on pontine growth cones, as they were susceptible to

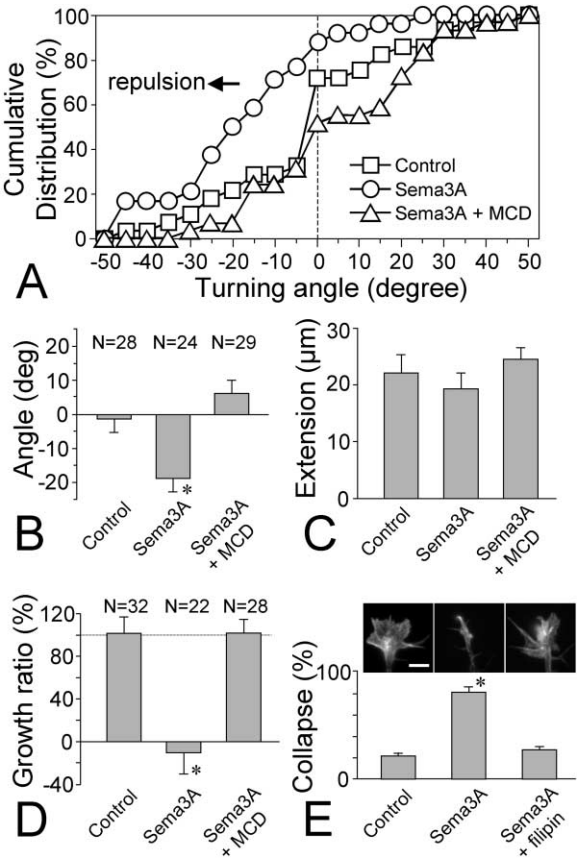

Figure 5. Lipid Rafts Mediate Sema3A-Induced Repulsion, Growth Inhibition, and Growth Cone Collapse

(A) The cumulative histogram shows the distribution of turning angles for growth cones exposed to control vehicle or Sema3A gradients with or without MCD treatment.

(B and C) The average turning angles (B) and net extension (C) for each group are presented in the bar graphs. Numbers in (B) indicate the total number of growth cones examined for each condition.

(D) Growth inhibition by bath application of Sema3A as analyzed by the growth assay.

(E) Sema3A-induced collapse of pontine growth cones. Pontine explant cultures were exposed to control vehicle or Sema3A with or without filipin treatment. The fluorescent images illustrate the representative growth cone actin cytoskeleton resulting from each condition. The scale bar equals 10 μm.

damage during MCD exposure. Taken together, these results indicate that lipid rafts mediate the inhibitory actions of the guidance molecule Sema3A in both *Xenopus* spinal neurons and mammalian CNS neurons.

Raft-Dependent Activation of p42/p44 MAPK in Guidance Responses

Our findings that lipid rafts mediate growth cone responses suggest a role for lipid rafts in signal transduction of guidance molecules. We therefore examined the raft dependence of p42/p44 MAPK activation by these cues (Campbell and Holt, 2003; Forcet et al., 2002; Ming et al., 2002). Using a specific antibody against phospho-p42/p44 and quantitative fluorescence imaging, we found that a brief exposure of *Xenopus* growth cones to BDNF, netrin-1, and Sema3A, but not glutamate, induced a large increase in p42/p44 phosphorylation, whereas no change in the total p42/p44 level was observed using a different antibody that recognizes total p42/p44 (Figures 6A and 6B). Treatment of *Xenopus* neurons with 5 mM MCD or 20 μM G_{M1} largely diminished the guidance cue-induced increase in p42/p44 phosphorylation without affecting the total p42/p44 level at the growth cone (Figures 6A and 6B). We also observed an asymmetric increase of p42/p44 phosphorylation across the growth cone subjected to the BDNF gradient, suggesting its role in growth cone turning (Figure 6C). We thus used a specific inhibitor PD98059 to block p42/p44 activation and examined the requirement of p42/p44 activation in the turning response. Consistent with previous findings (Campbell and Holt, 2003; Forcet et al., 2002; Ming et al., 2002), application of 10 μM PD98059 (30 min before the turning assay) largely blocked the turning responses to gradients of BDNF, netrin-1, and Sema3A, but did not affect glutamate-induced attraction (Figure 6D). These parallel results point to the involvement of raft-dependent p42/p44 activation in guidance responses of growth cones to BDNF, netrin-1, and Sema3A.

Association of Guidance Receptors with Lipid Rafts

The above findings make a strong case that lipid rafts are functionally involved in growth cone guidance and suggest that receptors for BDNF, netrin-1, and Sema3A, but not glutamate, are associated with lipid rafts and dependent on them for functioning. To test this possibility, we examined whether the BDNF receptor TrkB and the netrin-1 receptor DCC are localized in lipid rafts using standard membrane fractionation and Western blot methods (Kawabuchi et al., 2000). Due to the limited number of spinal neurons in *Xenopus* cultures, we used relatively pure cortical cultures from embryonic rats for the membrane fractionation experiments (Ma et al., 2003; Suzuki et al., 2001). We detected a small but prominent portion of DCC and TrkB in the lipid raft fraction as indicated by the lipid raft marker caveolin-2 (Cav-2; Figure 7A, lane 1; Simons and Toomre, 2000). Interestingly, a brief exposure of cortical neurons to BDNF (200 ng/ml, 30 min) before fractionation resulted in a noticeable increase in the amount of TrkB in the two most buoyant fractions, including the lipid raft fraction (Figure 7A). Netrin-1 exposure (200 ng/ml, 30 min) also increased the amount of DCC in the lipid raft fraction, although the increase was relatively small. Moreover, netrin-1 exposure increased the levels of DCC in fractions two through four (Figure 7A, lanes 2–4), suggesting a netrin-1-dependent translocation of DCC toward buoyant partitions. Collectively, these results indicate that guidance cues induced further association of their receptors with lipid rafts (Ma et al., 2003; Paratcha et al., 2001). Since this biochemical assay relies on membrane fractions from whole-cell lysates, it lacks the sensitivity to detect receptor-raft association at the growth cone. We thus used a more sensitive and well-established fluorescence copatching assay to examine raft association of specific guidance receptors on the surface of *Xenopus* growth cones (Harder et al., 1998; Simons and Toomre, 2000). This copatching method is based on

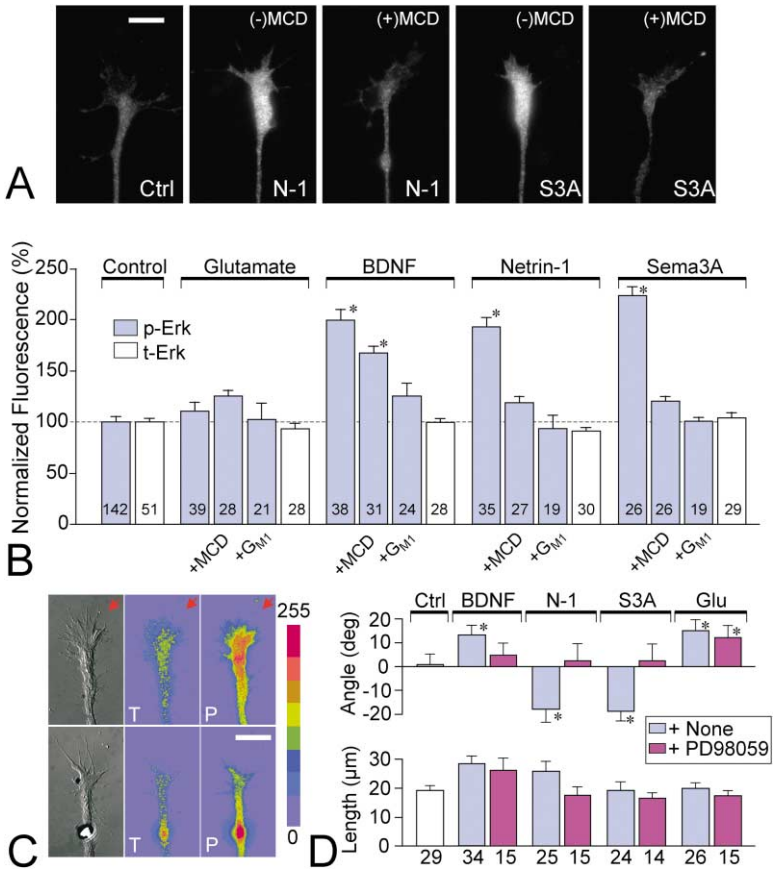

Figure 6. Raft-Dependent Activation of p42/p44 MAPK in Growth Cone Guidance

(A) Representative fluorescence images of *Xenopus* growth cones stained with a specific antibody against phospho-p42/p44. The growth cones were exposed to either control medium (Ctrl), netrin-1 (N-1), or Sema3A (S3A), without (−) or with (+) MCD treatment. Scale bar equals 10 μm.

(B) Levels of phospho-p42/p44 and total p42/p44 in *Xenopus* growth cones induced by different guidance cues, with or without lipid raft disruption by bath application of MCD or G_{M1}. Numbers denote the growth cones examined in each condition. Asterisks indicate statistical significance ($p < 0.01$, Student's t test).

(C) Local application of BDNF induced asymmetric activation of p42/p44. The top pair shows a *Xenopus* growth cone exposed to the BDNF gradient (arrows) for 5 min, fixed, and immunostained for total p42/p44 (T) and phospho-p42/p44 (P). For visualization, the intensity of the fluorescence images is coded by 8-level pseudocolors (see the color bar). The bottom pair shows a control growth cone without BDNF application.

(D) Inhibition of p42/p44 by PD98059 blocked turning responses. The average turning angles and neurite lengths are displayed as bar graphs. Numerals indicate the number of growth cones examined in each group.

the physical attraction among raft components whereby membrane proteins associated with lipid rafts can be crosslinked by antibodies to form patches that colocalize with raft patches formed by crosslinking G_{M1} gangliosides using cholera toxin B subunit (CTxB) (Harder et al., 1998). The raft association of a particular receptor can then be quantified by the percentage of receptor patches colocalizing with CTxB patches. We examined four receptors using this copatching method: NMDA receptor subunit 2B (NR2B), TrkB, DCC, and neuropilin-1 (NPN-1). We found that most patches of NR2B receptors did not colocalize with CTxB patches (Figures 7B and 7C), indicating the lack of raft association of NR2B (Suzuki et al., 2001; Wu et al., 1997). We therefore considered the percentage of NR2B patches colocalized with CTxB patches (~10%) as the baseline of the copatching method for significant raft association in our culture system. Consistent with the Western blot data (Figure 7A), only a small percentage of DCC, TrkB, and NPN-1 were associated with lipid rafts before ligand exposure (Figure 7C). However, a brief exposure to specific guidance cues (5 min) induced marked increase in the colocalization percentage of TrkB, DCC, and NPN-1 with raft patches (Figure 7C). In contrast, NMDA receptor patches did not exhibit any changes in colocalization with lipid rafts. These results illustrate that BDNF, netrin-1, and Sema3A, but not glutamate, increased the association of their respective receptors with lipid rafts and suggest the existence of ligand-induced receptor recruitment to lipid microdomains (Hering et al., 2003; Ma et al., 2003).

One immediate implication of the ligand-induced receptor-raft association is the generation of localized signaling that underlies directional responses of nerve growth cones in guidance gradients. A guidance gradient likely elicits more receptor-raft association on the *near* side of the growth cone where it is exposed to a higher concentration of the cue, thus creating an asymmetry for downstream signaling. To test this possibility, we used an in situ cold detergent extraction method to isolate membrane rafts and associated receptors on the growth cone. By double labeling raft marker G_{M1} and the specific receptor, we examined the spatial distribution of receptor-raft association on the growth cone. We selected BDNF for this study since our Western blot and copatching data showed a strong increase in TrkB-raft association after BDNF exposure. The growth cone was exposed to 3 min BDNF gradient and rapidly detergent-extracted and fixed by a prechilled solution containing Triton X-100 and fixative. The TrkB receptors were then immunostained and lipid rafts were labeled by staining G_{M1} with FITC-CTxB. Without cold detergent extraction, both G_{M1} and TrkB staining appeared to be homogenous across the growth cone surface (Figure 8A). Growth cones subjected to the cold detergent extraction displayed punctate staining of TrkB and G_{M1} and, most importantly, almost all the TrkB puncta overlapped with G_{M1} staining, indicating that these are detergent-resistant raft-associated TrkB receptors (hereafter referred to as *TrkB-raft*). For growth cones not exposed to the BDNF gradient, the TrkB-raft distribution appeared to be symmetric across the growth cone surface (Figure

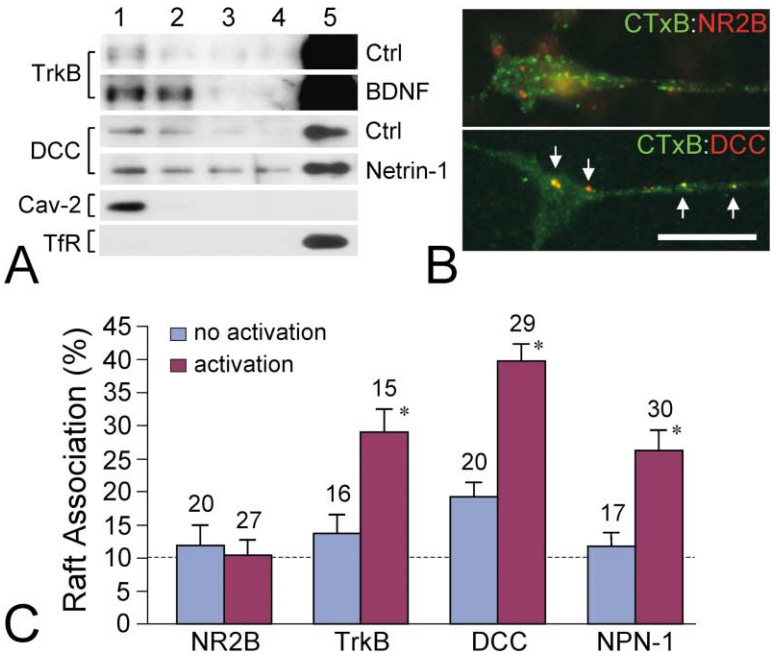

Figure 7. Association of Guidance Receptors with Lipid Rafts

(A) Immunoblots of membrane fractions from rat cortical neurons were probed with antibodies against TrkB or DCC. Lane numbers indicate the membrane fractions where 1 and 5 are the relative top to bottom fractions, respectively. Lane 1 represents the lipid raft fraction as indicated by the raft marker caveolin-2 (Cav-2), and lane 5 represents the nonraft fraction as indicated by transferrin receptors (TfR).

(B) Fluorescent copatching in *Xenopus* neurons. Representative fluorescent images show *Xenopus* growth cones with lipid raft patches induced by FITC-cholera toxin B subunit (CTxB, green) and receptor patches induced by antibodies against NR2B receptors (top) or DCC receptors (bottom). The receptor patches were further labeled by secondary antibody conjugated with Cy3 (red). Arrows indicate colocalized patches that appear yellow/orange. Scale bar equals 10 μm.

(C) Quantification of raft association of four different receptors by the copatching method on *Xenopus* neurons with or without ligand application. Asterisks indicate statistical significance when comparing between the groups without and with ligand exposure ($p < 0.01$, Student's t test).

8B). However, 3 min exposure of growth cones to the BDNF gradient resulted in a significant increase of TrkB-raft labeling on the *near* side of the growth cone relative to the *far* side (Figure 8C). Quantitative analysis of TrkB-raft staining on two sides of the growth cone revealed a 2:1 difference in TrkB-raft distribution (Figure 8D). These observations provide evidence that asymmetric receptor-raft association is induced by the guidance gradient and suggests a role for receptor-raft association in localized signaling in the growth cone during guidance responses.

Discussion

Increasing evidence suggests that cells utilize dynamic membrane microdomains (lipid rafts) to provide an ordered lipid microenvironment for specific molecular interactions between membrane receptors and distinct intracellular signaling components (Brown and London, 1998; Paratcha and Ibanez, 2002; Simons and Toomre, 2000; Tsui-Pierchala et al., 2002). Here we present evidence that lipid rafts selectively mediate growth cone guidance by BDNF, netrin-1, and Sema3A. This conclusion is based on results from the functional guidance assays coupled with lipid raft manipulation as well as biochemical and imaging studies on receptor-raft association. Several lines of evidence further support the selectivity of our raft manipulations in blocking guidance responses. First, acute cholesterol manipulation by two different molecules, MCD and filipin, did not drastically affect the growth cone's morphology or motility on the laminin substrate. These results also imply that growth cone motility on laminin (through β1 integrin) does not depend on lipid rafts (Nakai and Kamiguchi, 2002). Second, the consistent turning responses that resulted shortly after cholesterol rescue argue against the possibility that cholesterol extraction depleted membrane receptors and other proteins to affect guidance. Third, focal MCD application (in the absence of guidance cues) did not affect growth cone extension, further indicating that MCD does not influence general aspects of steering. Fourth, the abolishment of guidance responses by exogenous G_{M1} implicates the lipid microenvironment, not cholesterol itself, in mediating guidance responses. Finally, the fact that *Xenopus* growth cones subjected to lipid raft disruption still responded attractively to glutamate gradients provides, arguably, the best evidence that lipid rafts selectively mediate guidance actions of BDNF, netrin-1, and Sema3A.

Our examination of p42/p44 MAPK activation by BDNF, netrin-1, and Sema3A supports the notion that lipid rafts are involved in signal transduction. We found that either MCD or G_{M1} attenuated p42/p44 phosphorylation induced by these molecules. In particular, the increase in p42/p44 phosphorylation induced by netrin-1 and Sema3A was completely blocked by MCD or G_{M1}. BDNF-induced p42/p44 phosphorylation, on the other hand, was only reduced by MCD cholesterol extraction but effectively abolished by G_{M1} addition. While the exact mechanism underlying the difference between MCD and G_{M1} on inhibiting p42/p44 phosphorylation elicited by BDNF is not clear, these findings are consistent with MCD and G_{M1} effects on BDNF promotion of neurite extension. Further elucidation of the precise signaling pathways underlying these two BDNF effects would provide important insights toward the differential dependence on lipid rafts. Nevertheless, our results, together with the blockade of turning responses by MAPK inhibitors, suggest that raft-dependent p42/p44 activation underlies chemotropic actions of BDNF, netrin-1, and Sema3A.

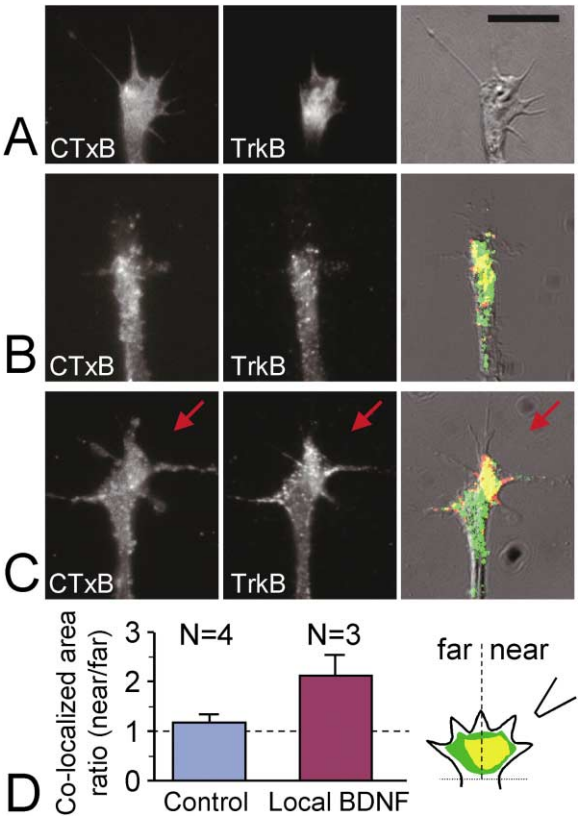

Figure 8. Asymmetric TrkB Receptor-Raft Association on the Growth Cone Surface Induced by BDNF Gradients

(A) A *Xenopus* growth cone fixed and double stained for surface G_{M1} by FITC-CTxB and TrkB receptors by immunostaining. The DIC image of the growth cone is shown on the right. Scale bar equals 10 μm.

(B) A *Xenopus* growth cone subjected to in situ cold detergent extraction and fixation. G_{M1} staining by FITC-CTxB and TrkB by immunostaining exhibited a punctate pattern. For quantification, each fluorescent image was set with a threshold (50% of the maximum intensity of the growth cone), pseudocolored (green for G_{M1} and red for TrkB), and overlaid on the DIC image. The yellow color indicates the overlapped area between G_{M1} and TrkB.

(C) A *Xenopus* growth cone subjected to the BDNF gradient (arrows) for 3 min before in situ cold detergent extraction/fixation and staining.

(D) Quantification of overlapped G_{M1} and TrkB on the two sides of the growth cone without (control) and with local BDNF exposure. The ratios are derived from the TrkB-raft colocalized areas on the two sides of the growth cone, each normalized against its respective G_{M1} staining area.

It is of interest to note that BDNF-elicited neurite extension and chemoattraction appear to depend on lipid rafts differently. While chemoattractive effects of BDNF were abolished by lipid raft disruption through MCD cholesterol extraction, the growth promotion was not affected, suggesting that growth promotion and chemoattraction are mechanistically separate events (Guirland et al., 2003; Markus et al., 2002; Ming et al., 1997, 1999). On the other hand, we find that BDNF-induced growth promotion was largely abolished by exogenous G_{M1} addition. BDNF is known to elicit multiple signaling cascades leading to diverse neuronal functions (Kaplan and Miller, 2000; Markus et al., 2002), thus it is conceivable that signaling cascades underlying chemoattraction and growth promotion may depend on different aspects of lipid microdomains on the membrane, which can be independently altered by cholesterol extraction and G_{M1} addition. Intriguingly, p42/p44 MAPK appears to be involved in both BDNF chemoattraction and growth promotion but differently affected by MCD and G_{M1}, which may be attributed to distinct spatiotemporal localization and/or intensity of MAPK signals. Contrary to the BDNF findings, we found that the growth inhibition, growth cone collapse, and growth cone repulsion induced by Sema3A all depended on lipid rafts and could be blocked by MCD treatment, suggesting a common signaling pathway but with distinct spatiotemporal regulation. For example, local Collapsin-1/Sema3A induced growth cone repulsion through local collapse of growth cone lamellipodia, while uniform Collapsin-1 caused the collapse of the whole growth cone and growth inhibition (Fan and Raper, 1995). Recent studies find that Sema3A signaling involves the formation of a complex consisting of neuropillin-1, plexin A, and the adhesion molecule L1 (Castellani and Rougon, 2002; Pasterkamp and Kolodkin, 2003). It has been reported that L1 is associated with lipid rafts and plays an important role in growth cone adhesion and migration (Nakai and Kamiguchi, 2002). Our findings thus indicate that lipid rafts mediate Sema3A signaling for distinct inhibitory actions.

How exactly are lipid rafts involved in the signal transduction of guidance cues? Several nonmutually exclusive models have been proposed (Simons and Toomre, 2000): (1) receptors can strongly associate with lipid rafts, (2) receptors can be recruited into lipid rafts upon ligand binding, leading to signal localization and amplification, and/or (3) rafts can be aggregated upon ligand binding to link particular receptors with distinct raft-dependent signaling complexes. Our Western blots and fluorescent copatching data indicate that receptors for the guidance cues studied here were weakly associated with lipid rafts under baseline conditions, but the receptor-raft association was markedly enhanced after stimulation by their respective ligands. It is possible that association of ligand-receptor complexes with lipid rafts enables the assembly of appropriate signaling complexes for guidance functions (Simons and Toomre, 2000; Tsui-Pierchala et al., 2002). For example, growth cone guidance by BDNF and netrin-1 involves phospholipase C (PLC) and PI-3 kinases (Ming et al., 1999), both of which associate with lipid rafts (Inoue et al., 2002). Many nonreceptor tyrosine kinases involved in adhesion are also associated with lipid rafts (Simons and Toomre, 2000), and active Rho-GTPases are targeted to lipid rafts for coupling to downstream effectors (del Pozo et al., 2004; Michaely et al., 1999; Palazzo et al., 2004). Therefore, lipid rafts may mediate growth cone guidance by providing a critical platform for localized coupling of activated receptors and/or their downstream effectors for cytoskeletal regulation.

A gradient of guidance cues is thought to activate surface receptors asymmetrically to generate localized responses that steer the growth cone in a particular direction. The local raft disruption data (see Figure 4) provide direct evidence that localized raft-dependent signaling is sufficient to initiate directional responses of growth cones. Previous studies on chemotactic cells

have shown that the overall distribution of membrane receptors for specific chemokines remains uniform during chemotaxis and localization of responses is downstream of membrane receptors (Parent and Devreotes, 1999). Exactly how is such localization generated through uniformly distributed surface receptors? We propose that an asymmetry in lipid raft association of the guidance receptor, without apparent changes in overall distribution, represents the first step of signal localization during directional responses. In particular, the asymmetric translocation of guidance receptors into lipid rafts after ligand binding could lead to local signal amplification by concentrating signaling molecules and/or excluding unwanted modulatory components (Simons and Toomre, 2000), which might be essential for successful sensing of extracellular gradients. Our observation of asymmetric TrkB-raft distribution on growth cones exposed to BDNF gradients provides evidence to support this local signaling model. Future experiments involving high-resolution imaging such as fluorescence resonance energy transfer (FRET) would provide detailed insights into the spatiotemporal interactions of signaling components across the growth cone surface during guidance.

One of the important findings in this study is the involvement of lipid rafts in inhibitory and collapsing effects of Sema3A. One can postulate that lipid rafts may also be involved in signaling by other inhibitory molecules. For example, p75 receptors have recently been identified as the coreceptors for growth inhibitory molecules including myelin-associated glycoprotein (MAG) and NOGO (Wang et al., 2002a; Wong et al., 2002) and are known to associate with lipid rafts (Bilderback et al., 1997). Furthermore, MAG has been shown to interact with specific lipid gangliosides (Vyas et al., 2002), and the GPI-linked NOGO receptor may partition in lipid rafts for its functions (Wang et al., 2002b). It is conceivable that lipid rafts play a major role in MAG/NOGO inhibition of axonal growth. Since growth inhibition represents a major barrier for nerve regeneration in the adult nervous system, our results are of particular interest as they identify lipid rafts as a potential target for further determination of signaling components responsible for inhibition. Moreover, the finding that disruption of lipid rafts abolishes Sema3A-induced inhibition suggests that manipulation of lipid raft integrity or individual lipid raft components could be an effective approach to overcoming growth inhibition. Clearly, a deeper understanding of the specific guidance receptors, signaling components, and kinetics with which they are recruited to lipid rafts to interact with other signaling components would provide invaluable insights into mechanisms underlying the precise wiring of complex neuronal connections. Importantly, such an understanding can contribute to novel strategies of enhancing nerve regeneration after injury that specifically rely on manipulation of lipid rafts and their associated components.

Experimental Procedures

Xenopus Culture, Turning Assay, and Focal Application

Xenopus cultures and turning assays are described previously (Guirland et al., 2003) except assays were done in a modified Ringer's solution (Ming et al., 1999). We used the nonparametric Mann-Whitney test to analyze turning angles since they do not follow a normal distribution. Focal application of MCD was achieved by a modified pipette application method (Buck and Zheng, 2002). Glutamate was purchased from Sigma. Human recombinant BDNF (rHu-met-BDNF) was generously provided by Regeneron (Tarrytown, NY). Purified netrin-1 proteins were a gift from Dr. Marc Tessier-Lavigne (Genetech). Sema3A was collected from the supernatant of confluent COS cells expressing human Sema3A (Kolodkin et al., 1993) and dialyzed into Ringer's saline for pipette application. The vehicle control solution was obtained from the supernatant of mock-transfected COS cells that expressed the same vector lacking the hSema3A insert. Methyl-β-cyclodextrin, filipin, and G_{M1} gangliosides were purchased from Sigma and were added to the bath medium 20–30 min before the onset of turning assay.

Pontine Explant Culture and Collapse Assay

Pontine nuclei explants were prepared as described previously (Baird et al., 1992). Collapse assays were performed on cultures with or without filipin pretreatment (1 μg/ml, 25 min) by incubating them with Sema3A or the vehicle control solutions for 30 min. The Sema3A stock solution (described above) was added at a 1:20 dilution, which resulted in ~80% collapse of pontine growth cones (Rabacchi et al., 1999). The vehicle stock solution was also used at the same dilution. Explants were then quickly fixed with 4% paraformaldehyde and 0.25% glutaraldehyde in a cacodylate buffer (Guirland et al., 2003) for 30 min, permeabilized with Triton X-100 (0.1%), and labeled with rhodamine-phalloidin (1.5%; Molecular Probes) for 15 min. Fluorescence imaging was performed on a Nikon inverted microscope (TE2000) equipped with a 40× Plan Fluor oil-immersion objective (numeric aperture: 1.3), a CCD camera (PXL1400, Roper Scientific), and Axon Imaging Workbench software (Axon Instruments). Images were analyzed for percentages of collapsed growth cones.

Quantitative Imaging of Phospho-p42/p44 and p42/p44

Xenopus cultures, treated with or without 5 mM MCD or 20 μM G_{M1} (30 min), were exposed to glutamate (50 μM), BDNF (50 ng/ml), netrin-1 (200 ng/ml), Sema3A (1:20), or control medium for 5 min. The cells were then fixed as above for 10 min, permeabilized, and labeled with antibodies against phospho-p42/44 or total p42/p44 (Cell Signaling Technology, Boston, MA) and Cy3-conjugated secondary antibodies (Jackson ImmunoResearch). Imaging was done using a 60×/1.4 Plan Apo objective with the same settings between the control and exposed groups. Background subtracted images were analyzed by creating a region of interest (ROI) that was circumscribed by the growth cone. For each growth cone, the ROI intensity was normalized to the average from the parallel control. Data for each condition were from at least two separate batches of *Xenopus* cultures. To assess asymmetric activation of p42/p44, the growth cone was subjected to 5 min BDNF pipette application (50 μm from the growth cone) and then rapidly fixed, stained, and imaged. We double stained the total and phopho-p42/44 using a polyclonal anti-p42/p44 and a monoclonal anti-phospho-p42/p44 (Cell Signaling), followed by FITC- and Cy3-conjugated secondary antibodies. Each channel of the staining was acquired using the same parameters and saved for further processing and analysis.

Membrane Fractionation and Immunoblots

Membrane fractions were prepared from cultured cortical neurons (Ma et al., 2003; Suzuki et al., 2001) as described previously (Kawabuchi et al., 2000). Six membrane fractions were collected from the top of the gradient with the second fraction containing caveolin-2 (Cav-2), thus designated as the lipid raft fraction (Figure 7A, lane 1), and the last fraction containing transferrin receptor (TfR), therefore designated as the nonraft fraction (Figure 7A, lane 5). The six fractions were then subjected to SDS-PAGE and probed with antibodies for TrkB receptor (BD Biosciences), DCC (Santa Cruz), or caveolin-2 (BD Biosciences) using a standard immunoblot procedure (Kawabuchi et al., 2000).

Fluorescent Copatching of Lipid Rafts and Membrane Receptors

We adapted the previously described patching method (Harder et al., 1998) for *Xenopus* neurons. Briefly, membrane rafts and recep-

tors were clustered by FITC-conjugated cholera toxin B subunit (CTxB; 8 μg/ml; Sigma) and an appropriate primary antibody for 1 hr at 12°C, followed by a Cy3-labeled secondary antibody for 45 min at 12°C. The cells were then fixed in 4% paraformaldehyde and 0.25% glutaraldehyde for 4 min, followed by cold MeOH for 5 min. Digital images of both green (FITC) and red (Cy3) channels of each neuron were individually acquired, background subtracted, and merged as separate layers using Adobe Photoshop (Adobe Systems). We quantified the raft association on the growth cone and adjacent neurite shafts by determining the percentage of receptor clusters colocalized with G_{M1} patches. Antibodies were rabbit against NR2B (Upstate Biotechnology), chicken IgY against TrkB extracellular domain (kindly supplied by L. Reichardt), mouse against DCC (Oncogene), and rabbit against NPN-1 (generously provided by Dr. David Ginty).

In Situ Cold Detergent Extraction and Fixation

Xenopus growth cones were first exposed to BDNF gradients for 3 min (100 μM in pipette, 50 μm away, 10 ms pulse duration), immediately subjected to simultaneous cold detergent extraction and fixation using an ice-cold cacodylate buffer containing triton X-100 (0.05%) and paraformaldehyde (2%) on ice for 5 min. After staining G_{M1} and TrkB, images of both channels were acquired and a threshold (50% of the maximum intensity of the growth cone) was set for each image to generate two color images (red, TrkB; green, CTxB), which were then merged and overlaid on its corresponding DIC image. To analyze the degree of asymmetric localization of TrkB to lipid rafts, we divided the growth cone into *near* and *far* halves with respect to the pipette (for control cells, *near* was the right hand side), measured the yellow area (TrkB localized with G_{M1}), and normalized it against the green area (G_{M1} staining by FITC-CTxB) in each half of the growth cone. The area ratio of the growth cone (*near/far*) was simply calculated from the normalized values and an even distribution of TrkB-raft produces a ratio of 1.

Acknowledgments

We thank Dr. Marc Tessier-Lavigne at Genetech for providing purified netrin-1 proteins, Dr. Corey Goodman at UC Berkeley for supplying Sema3A-expressing COS cells, and Dr. David Ginty at John Hopkins Medical School for sharing the anti-neuropilin-1 antibodies. We are also grateful to Dr. Donald Winkelemann (Department of Pathology, UMDNJ-RWJMS) for imaging assistance and Dr. Kuo Wu (Department of Neuroscience and Cell Biol., UMDNJ-RWJMS) for help in immunostaining. This work is supported by a grant from National Institutes of Health.

Received: June 18, 2003
Revised: November 18, 2003
Accepted: March 2, 2004
Published: April 7, 2004

References

Baird, D.H., Baptista, C.A., Wang, L.C., and Mason, C.A. (1992). Specificity of a target cell-derived stop signal for afferent axonal growth. J. Neurobiol. *23*, 579–591.

Bilderback, T.R., Grigsby, R.J., and Dobrowsky, R.T. (1997). Association of p75(NTR) with caveolin and localization of neurotrophin-induced sphingomyelin hydrolysis to caveolae. J. Biol. Chem. *272*, 10922–10927.

Brown, D.A., and London, E. (1998). Functions of lipid rafts in biological membranes. Annu. Rev. Cell Dev. Biol. *14*, 111–136.

Buck, K.B., and Zheng, J.Q. (2002). Growth cone turning induced by direct local modification of microtubule dynamics. J. Neurosci. *22*, 9358–9367.

Campbell, D.S., and Holt, C.E. (2003). Apoptotic pathway and MAPKs differentially regulate chemotropic responses of retinal growth cones. Neuron *37*, 939–952.

Castellani, V., and Rougon, G. (2002). Control of semaphorin signaling. Curr. Opin. Neurobiol. *12*, 532–541.

del Pozo, M.A., Alderson, N.B., Kiosses, W.B., Chiang, H.H., Anderson, R.G., and Schwartz, M.A. (2004). Integrins regulate Rac targeting by internalization of membrane domains. Science *303*, 839–842.

Fan, J., and Raper, J.A. (1995). Localized collapsing cues can steer growth cones without inducing their full collapse. Neuron *14*, 263–274.

Forcet, C., Stein, E., Pays, L., Corset, V., Llambi, F., Tessier-Lavigne, M., and Mehlen, P. (2002). Netrin-1-mediated axon outgrowth requires deleted in colorectal cancer-dependent MAPK activation. Nature *417*, 443–447.

Guirland, C., Buck, K.B., Gibney, J.A., DiCicco-Bloom, E., and Zheng, J.Q. (2003). Direct cAMP signaling through G-protein-coupled receptors mediates growth cone attraction induced by pituitary adenylate cyclase- activating polypeptide. J. Neurosci. *23*, 2274–2283.

Harder, T., Scheiffele, P., Verkade, P., and Simons, K. (1998). Lipid domain structure of the plasma membrane revealed by patching of membrane components. J. Cell Biol. *141*, 929–942.

Hering, H., Lin, C.C., and Sheng, M. (2003). Lipid rafts in the maintenance of synapses, dendritic spines, and surface AMPA receptor stability. J. Neurosci. *23*, 3262–3271.

Hong, K., Nishiyama, M., Henley, J., Tessier-Lavigne, M., and Poo, M. (2000). Calcium signalling in the guidance of nerve growth by netrin-1. Nature *403*, 93–98.

Hopker, V.H., Shewan, D., Tessier-Lavigne, M., Poo, M., and Holt, C. (1999). Growth-cone attraction to netrin-1 is converted to repulsion by laminin- *1*. Nature *401*, 69–73.

Huber, A.B., Kolodkin, A.L., Ginty, D.D., and Cloutier, J.F. (2003). Signaling at the growth cone: ligand-receptor complexes and the control of axon growth and guidance. Annu. Rev. Neurosci. *26*, 509–563.

Ilangumaran, S., and Hoessli, D.C. (1998). Effects of cholesterol depletion by cyclodextrin on the sphingolipid microdomains of the plasma membrane. Biochem. J. *335*, 433–440.

Inoue, H., Miyaji, M., Kosugi, A., Nagafuku, M., Okazaki, T., Mimori, T., Amakawa, R., Fukuhara, S., Domae, N., Bloom, E.T., and Umehara, H. (2002). Lipid rafts as the signaling scaffold for NK cell activation: tyrosine phosphorylation and association of LAT with phosphatidylinositol 3- kinase and phospholipase C-gamma following CD2 stimulation. Eur. J. Immunol. *32*, 2188–2198.

Kaplan, D.R., and Miller, F.D. (2000). Neurotrophin signal transduction in the nervous system. Curr. Opin. Neurobiol. *10*, 381–391.

Kawabuchi, M., Satomi, Y., Takao, T., Shimonishi, Y., Nada, S., Nagai, K., Tarakhovsky, A., and Okada, M. (2000). Transmembrane phosphoprotein Cbp regulates the activities of Src-family tyrosine kinases. Nature *404*, 999–1003.

Kolodkin, A.L., Matthes, D.J., and Goodman, C.S. (1993). The semaphorin genes encode a family of transmembrane and secreted growth cone guidance molecules. Cell *75*, 1389–1399.

Ma, L., Huang, Y.Z., Pitcher, G.M., Valtschanoff, J.G., Ma, Y.H., Feng, L.Y., Lu, B., Xiong, W.C., Salter, M.W., Weinberg, R.J., and Mei, L. (2003). Ligand-dependent recruitment of the ErbB4 signaling complex into neuronal lipid rafts. J. Neurosci. *23*, 3164–3175.

Markus, A., Patel, T.D., and Snider, W.D. (2002). Neurotrophic factors and axonal growth. Curr. Opin. Neurobiol. *12*, 523–531.

McKerracher, L., and Winton, M.J. (2002). Nogo on the go. Neuron *36*, 345–348.

Michaely, P.A., Mineo, C., Ying, Y.S., and Anderson, R.G. (1999). Polarized distribution of endogenous Rac1 and RhoA at the cell surface. J. Biol. Chem. *274*, 21430–21436.

Ming, G.L., Lohof, A.M., and Zheng, J.Q. (1997). Acute morphogenic and chemotropic effects of neurotrophins on cultured embryonic *Xenopus* spinal neurons. J. Neurosci. *17*, 7860–7871.

Ming, G., Song, H., Berninger, B., Inagaki, N., Tessier-Lavigne, M., and Poo, M. (1999). Phospholipase C-gamma and phosphoinositide 3-kinase mediate cytoplasmic signaling in nerve growth cone guidance. Neuron *23*, 139–148.

Ming, G., Henley, J., Tessier-Lavigne, M., Song, H., and Poo, M.

(2001). Electrical activity modulates growth cone guidance by diffusible factors. Neuron *29*, 441–452.

Ming, G.L., Wong, S.T., Henley, J., Yuan, X.B., Song, H.J., Spitzer, N.C., and Poo, M.M. (2002). Adaptation in the chemotactic guidance of nerve growth cones. Nature *417*, 411–418.

Nakai, Y., and Kamiguchi, H. (2002). Migration of nerve growth cones requires detergent-resistant membranes in a spatially defined and substrate-dependent manner. J. Cell Biol. *159*, 1097–1108.

Palazzo, A.F., Eng, C.H., Schlaepfer, D.D., Marcantonio, E.E., and Gundersen, G.G. (2004). Localized stabilization of microtubules by integrin- and FAK-facilitated Rho signaling. Science *303*, 836–839.

Paratcha, G., and Ibanez, C.F. (2002). Lipid rafts and the control of neurotrophic factor signaling in the nervous system: variations on a theme. Curr. Opin. Neurobiol. *12*, 542–549.

Paratcha, G., Ledda, F., Baars, L., Coulpier, M., Besset, V., Anders, J., Scott, R., and Ibanez, C.F. (2001). Released GFRalpha1 potentiates downstream signaling, neuronal survival, and differentiation via a novel mechanism of recruitment of c-Ret to lipid rafts. Neuron *29*, 171–184.

Parent, C.A., and Devreotes, P.N. (1999). A cell's sense of direction. Science *284*, 765–770.

Pasterkamp, R.J., and Kolodkin, A.L. (2003). Semaphorin junction: making tracks toward neural connectivity. Curr. Opin. Neurobiol. *13*, 79–89.

Rabacchi, S.A., Solowska, J.M., Kruk, B., Luo, Y., Raper, J.A., and Baird, D.H. (1999). Collapsin-1/semaphorin-III/D is regulated developmentally in Purkinje cells and collapses pontocerebellar mossy fiber neuronal growth cones. J. Neurosci. *19*, 4437–4448.

Robinson, J.M., and Karnovsky, M.J. (1980). Evaluation of the polyene antibiotic filipin as a cytochemical probe for membrane cholesterol. J. Histochem. Cytochem. *28*, 161–168.

Simons, K., and Toomre, D. (2000). Lipid rafts and signal transduction. Nat. Rev. Mol. Cell Biol. *1*, 31–39.

Simons, M., Friedrichson, T., Schulz, J.B., Pitto, M., Masserini, M., and Kurzchalia, T.V. (1999). Exogenous administration of gangliosides displaces GPI-anchored proteins from lipid microdomains in living cells. Mol. Biol. Cell *10*, 3187–3196.

Song, H.J., Ming, G.L., and Poo, M.M. (1997). cAMP-induced switching in turning direction of nerve growth cones. Nature *388*, 275–279.

Stein, E., and Tessier-Lavigne, M. (2001). Hierarchical organization of guidance receptors: silencing of netrin attraction by slit through a Robo/DCC receptor complex. Science *291*, 1928–1938.

Suzuki, T., Ito, J., Takagi, H., Saitoh, F., Nawa, H., and Shimizu, H. (2001). Biochemical evidence for localization of AMPA-type glutamate receptor subunits in the dendritic raft. Brain Res. Mol. Brain Res. *89*, 20–28.

Tessier-Lavigne, M., and Goodman, C.S. (1996). The molecular biology of axon guidance. Science *274*, 1123–1133.

Tsui-Pierchala, B.A., Encinas, M., Milbrandt, J., and Johnson, E.M., Jr. (2002). Lipid rafts in neuronal signaling and function. Trends Neurosci. *25*, 412–417.

Vyas, A.A., Patel, H.V., Fromholt, S.E., Heffer-Lauc, M., Vyas, K.A., Dang, J., Schachner, M., and Schnaar, R.L. (2002). Gangliosides are functional nerve cell ligands for myelin-associated glycoprotein (MAG), an inhibitor of nerve regeneration. Proc. Natl. Acad. Sci. USA *99*, 8412–8417.

Wang, K.C., Kim, J.A., Sivasankaran, R., Segal, R., and He, Z. (2002a). P75 interacts with the Nogo receptor as a co-receptor for Nogo, MAG and OMgp. Nature *420*, 74–78.

Wang, K.C., Koprivica, V., Kim, J.A., Sivasankaran, R., Guo, Y., Neve, R.L., and He, Z. (2002b). Oligodendrocyte-myelin glycoprotein is a Nogo receptor ligand that inhibits neurite outgrowth. Nature *417*, 941–944.

Wong, S.T., Henley, J.R., Kanning, K.C., Huang, K.H., Bothwell, M., and Poo, M.M. (2002). A p75(NTR) and Nogo receptor complex mediates repulsive signaling by myelin-associated glycoprotein. Nat. Neurosci. *5*, 1302–1308.

Wu, C., Butz, S., Ying, Y., and Anderson, R.G. (1997). Tyrosine kinase receptors concentrated in caveolae-like domains from neuronal plasma membrane. J. Biol. Chem. *272*, 3554–3559.

Zheng, J.Q. (2000). Turning of nerve growth cones induced by localized increases in intracellular calcium ions. Nature *403*, 89–93.

Zheng, J.Q., Felder, M., Connor, J.A., and Poo, M.M. (1994). Turning of nerve growth cones induced by neurotransmitters. Nature *368*, 140–144.

Zheng, J.Q., Wan, J.J., and Poo, M.M. (1996). Essential role of filopodia in chemotropic turning of nerve growth cone induced by a glutamate gradient. J. Neurosci. *16*, 1140–1149.